ORIGINAL ARTICLE

Biological nitrogen fixation in the oxygen-minimum region of the eastern tropical North Pacific ocean

Amal Jayakumar[1], Bonnie X Chang[2,3], Brittany Widner[4], Peter Bernhardt[4], Margaret R Mulholland[4] and Bess B Ward[1]

[1]Department of Geosciences, Princeton University, Princeton, NJ, USA; [2]Joint Institute for the Study of the Atmosphere and Ocean, University of Washington, Seattle, WA, USA; [3]NOAA/Pacific Marine Environmental Laboratory, Seattle, WA, USA and [4]Department of Ocean, Earth and Atmospheric Sciences, Old Dominion University, Norfolk, VA, USA

Biological nitrogen fixation (BNF) was investigated above and within the oxygen-depleted waters of the oxygen-minimum zone of the Eastern Tropical North Pacific Ocean. BNF rates were estimated using an isotope tracer method that overcame the uncertainty of the conventional bubble method by directly measuring the tracer enrichment during the incubations. Highest rates of BNF ($\sim$4 nM day^{-1}) occurred in coastal surface waters and lowest detectable rates ($\sim$0.2 nM day^{-1}) were found in the anoxic region of offshore stations. BNF was not detectable in most samples from oxygen-depleted waters. The composition of the N_2-fixing assemblage was investigated by sequencing of *nifH* genes. The diazotrophic assemblage in surface waters contained mainly Proteobacterial sequences (Cluster I *nifH*), while both Proteobacterial sequences and sequences with high identities to those of anaerobic microbes characterized as Clusters III and IV type *nifH* sequences were found in the anoxic waters. Our results indicate modest input of N through BNF in oxygen-depleted zones mainly due to the activity of proteobacterial diazotrophs.
The ISME Journal (2017) **11**, 2356–2367; doi:10.1038/ismej.2017.97; published online 25 July 2017

Introduction

The balance between nitrogen (N) losses via deni-trification (including anammox) and inputs via biological dinitrogen (N_2) fixation (BNF), along with physical fluxes, determines the fixed N inventory of the ocean. BNF has traditionally been associated with the euphotic zone of oligotrophic regions while denitrification occurs in the absence of oxygen in both the water column and sediments.

Oxygen-minimum zones (OMZs), where dissolved oxygen is undersaturated relative to surrounding waters, occur across all ocean basins as the result of respiration of organic matter. Only in a few regions, which we refer to as oxygen-depleted zones (ODZs), are oxygen concentrations low enough to induce anaerobic metabolisms. It has long been recognized that ODZs are major sites for net N loss from the ocean. It has also been argued that, owing to the relative decrease in N availability associated with these N losses, the low oxygen concentrations (Mulholland and Capone, 2009; Großkopf and Laroche, 2012), and the relatively high available iron concentrations in ODZs, N_2 fixation should also

be favored in ODZs (Deutsch *et al.*, 2007; Mulholland and Capone, 2009). Efforts to test this idea have focused on the Eastern Tropical South Pacific (ETSP) ODZ, one of the three major oceanic ODZs, which together account for up to one-third of the global marine fixed N loss (Devol, 2008). Recent expeditions have reported BNF in both surface and deeper (anoxic) waters of this region (Fernandez *et al.*, 2011; Bonnet *et al.*, 2013; Dekaezemacker *et al.*, 2013; Loescher *et al.*, 2014) and have described diverse assemblages of diazotrophic microbes on the basis of their *nifH* genes (Loescher *et al.*, 2014; Turk-Kubo *et al.*, 2014). These studies reported anoxic BNF rates of up to 25 nM day^{-1} (Loescher *et al.*, 2014), which could contribute significantly to overall global BNF rates, and detected novel groups of previously unknown diazotrophic microbes, distinct from the well-known cyanobacterial N_2 fixers.

Global marine N budgets generally assume that biological N loss and input processes are roughly balanced, but such budgets contain large uncertain-ties, beginning with the methods used to make direct rate measurements of the processes and the paucity of such data. Recent improvements in the methods used to measure the rates of both N loss and N_2 fixation have greatly expanded the global data sets for these two major pathways in the N cycle. The exetainer method for measuring denitrification and anammox (Thamdrup and Dalsgaard, 2002) facili-tated the direct measurement of N losses from the

ocean while the bubble method for N_2 fixation (Montoya *et al.*, 1996) did the same for the measurement of BNF rates in many regions of the world ocean. However, the conventional bubble method can underestimate BNF rates by a variable amount (Mohr *et al.*, 2010; Großkopf *et al.*, 2012). This uncertainty complicates the extrapolation of direct rate measurements of N_2 fixation for comparison with geochemical estimates of this important global N budget term.

The goal of the present study was to investigate the distribution and magnitude of BNF in the Eastern Tropical North Pacific Ocean (ETNP), where much less is known about N losses and N_2 fixation than in the ETSP. In and around the ETNP ODZ, we quantified BNF using an improved method that overcomes the uncertainty of the bubble method and avoids perturbation of natural water samples with equilibrated enriched seawater. We also examined the phylogenetic composition of the N_2-fixing assemblage by sequencing cloned *nifH* genes from both surface and anoxic waters.

Materials and methods

Water samples were collected from multiple casts at each of the two stations, nearshore Station BB1 and offshore Station BB2, in the ETNP (Figure 1) during March and April of 2012 aboard the *R/V Thomas G. Thompson*. Casts 108, 110, 111, 120 and 124 were all at Station BB1 and Casts 138, 146 and 151 were all at BB2. Additional samples were collected at another nearshore station (Cast 103), on a transect perpendicular to the coast (Casts 134 and 163) and along a meridional transect along 110°W (Casts 168, 173 and 179) (Figure 1). High-resolution water-column nitrate, nitrite and oxygen concentrations at Stations BB1 and BB2 were reported previously (Peng *et al.*, 2015).

Water for BNF incubations was collected in triplicate from Niskin bottles (General Oceanics, Miami, FL, USA) mounted on a CTD rosette (SeaBird Electronics, Bellevue, WA, USA). Euphotic zone samples were collected from predawn casts and incubated in 2.5 l transparent polycarbonate bottles fitted with septa caps. Incubation bottles were placed in flow-through incubators on deck where temperature was maintained with flowing surface seawater and *in situ* light levels, estimated from the CTD PAR data, were simulated using neutral density screens.

ODZ samples were incubated in transparent acid-washed (10% HCl), helium-purged, evacuated, 2-mil-thick polyvinyl fluoride gas-tight 5 l Tedlar bags (Cole Parmer, Vernon Hills, IL, USA) with dual entry points: one a nickel-plated brass hose barb and the other a septum (Cole Parmer, Vernon Hills, IL, USA, EW-01409-92). Samples were transferred into the bags directly from the Niskin bottle using inert tubing attached to the hose barb, and remaining helium was removed from the bags via syringe
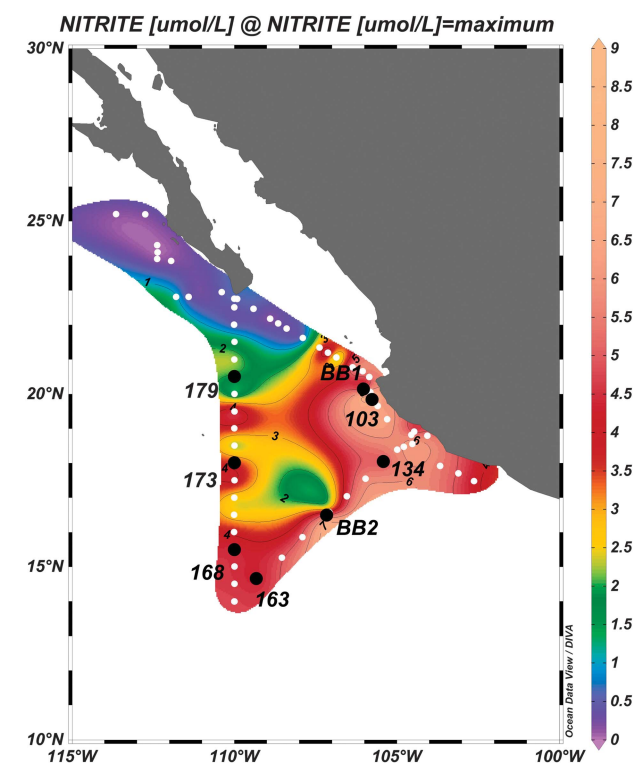

Figure 1 Map of station locations. Station BB1 includes Casts 108, 110, 111, 120 and 124. Station BB2 includes Casts 138, 146 and 151. White dots indicate stations on the cruise track that were used to derive the background contours of maximum NO_2^- concentration, which defines the oxygen-depleted water in the OMZ region.

attached to the septum during filling. Atmospheric O_2 contamination during water collection was minimized by continually flushing the head-space of the Niskin bottles with He gas. ODZ samples were incubated in a cold van (12 °C) in the dark (*in situ* temperature 12–13 °C).

$^{15}N_2$ tracer (99%, Cambridge Isotope Labs, Tewksbury, MA, USA) was injected into bottles and bags through the septa to a target concentration of ~10% ambient N_2. The duration of all incubations was ~24 h in order to capture the full diel light cycle in euphotic waters, where many diazotrophs exhibit diurnal cycles of N_2 fixation (Zehr *et al.*, 2007). Incubations were terminated by filtering the entire contents of the incubations onto precombusted (450 °C for 2 h) GF/F filters (Whatman, UK) (nominal pore size 0.7 μm). Filters were stored at −20°C, then dried and pelletized in tin discs and analyzed for isotopic enrichment on a Europa Geo 20/20 isotope ratio mass spectrometer (Little Chalfont, Buckinghamshire, UK) equipped with an automated nitrogen and carbon analyzer. To characterize and correct for the effect of a nonlinear detector response to varying sample size, known standards of different sample masses were run, bracketing the expected sample mass (Mcilvin and Casciotti, 2010). Samples to determine the initial isotopic composition of particulate organic matter in incubations were collected in triplicate on GF/F filters.

Rates of BNF were calculated using Equation (1):

$$\text{N}_2 \text{ fixation rate} = \frac{\left(A_{\text{PN}}^{\text{final}} - A_{\text{PN}}^{t=0}\right)}{\left(A_{\text{N}_2} - A_{\text{PN}}^{t=0}\right)} \times \frac{[\text{PN}]}{\Delta t} \quad (1)$$

where $A = $ atom% ^{15}N measured in the particulate organic N (PN) at the end (final) or beginning ($t = 0$) of the incubation or in the dissolved N_2 pool (N_2) (Montoya *et al.*, 1996; Mulholland *et al.*, 2006).

The method detection limit was calculated using the method of Santoro *et al.* (2013), except that we used $3\times$, instead of $2\times$, of the instrument s.d. to compute the limit. That is, the s.d. of the atom percent from seven standards of $12\,\mu\text{g N}$ each (0.0025%) was multiplied by three and added to the initial atom percent measurement for each sample. This was the minimum detectable final particulate atom percent enrichment (Analytical Detection Limit Guidance & Laboratory Guide for Determining Method Detection Limits, Wisconsin Department of Natural Resources Laboratory Certification Program, April 1996, PUBL-TS-056-96). This value was then forced through the calculation for each measurement to account for variability in particulate nitrogen concentrations with depth and incubation times, resulting in an independent detection limit for each measurement. The mean detection limit was $1.0\,\text{nmol N l}^{-1}\,\text{day}^{-1}$. The average detection limit for oxic incubations was substantially higher than for anoxic incubations (1.4 and $0.5\,\text{nmol N l}^{-1}\,\text{day}^{-1}$, respectively), due to large differences in particulate nitrogen concentrations between samples. Only rates above the detection limit (ADL) for that specific measurement are considered significant.

In order to estimate the change in atom% ^{15}N of the substrate N_2 pool over time due to gradual equilibration of the $^{15}\text{N}_2$ gas bubble, parallel incubations were carried out, in duplicate, using filtered seawater held at four different temperatures in a range approximating *in situ* temperatures (5–18.5 °C). The incubations were subsampled at 2 h intervals for the first 10 h and 4–6 h intervals thereafter (up to 24 h) into He-purged 12 ml Exetainers (Labco, Lampeter, UK), which were immediately poisoned with $0.05\,\text{ml}\ 7\,\text{M}\ \text{ZnCl}_2$. Exetainers were analyzed for atom% $^{15}\text{N}_2$ on a Europa 20/20 isotope ratio mass spectrometer. Separate polynomials for each temperature were fit to the resultant time-dependent equilibration curves. Each polynomial was integrated from 0 to 24 h and the result was divided by 24 to estimate the average atom% $^{15}\text{N}_2$ in sample incubations over the course of a 24-h incubation. Average atom% $^{15}\text{N}_2$ ranged from 3.9% at 5 °C to 5.5% at 18.5 °C (see Supplementary Figure).

DNA/RNA sequence analysis
Particulate material from five depths was collected for *nifH* sequence analysis: near surface (0 m), chlorophyll maximum (18 m), and secondary nitrite maximum (SNM, 90 m) at Station BB1 and near surface (0 m) and SNM (150 m) at Station BB2. Whole water (4–8 l) from CTD-mounted Niskin bottles was filtered through Sterivex-GP capsule filters (Millipore, Inc., Bedford, MA, USA), using a peristaltic pump, quick frozen in liquid nitrogen and shipped in liquid nitrogen to Princeton University. The samples were stored at −80 °C until DNA/RNA was extracted.

DNA and RNA were simultaneously extracted from Sterivex filters using the ALLPrep DNA/RNA Mini Kit (Qiagen Sciences, Germantown, MD, USA). cDNA was synthesized immediately following purification of RNA using a SuperScript III First Strand Synthesis System (Invitrogen, Carlsbad, CA, USA) following the procedure described by the manufacturer, including RT controls. DNA was quantified using the PicoGreen dsDNA Quantification Kit (Invitrogen) according to the manufacturer's specifications. *nifH* sequences were amplified from environmental DNA and cDNA using the Promega PCR Kit (Promega, Madison, WI, USA), on an MJ100 Thermal Cycler (MJ Research, Watertown, MA, USA). A nested reaction was used, as previously described (Zehr *et al.*, 1998), with slight modification: 25 μl PCR reactions were amplified for 30 cycles (1 min at 98 °C, 1 min at 57 °C, 1 min at 72 °C), first with the outer PCR primers (Zani *et al.*, 2000), followed by amplification with the inner PCR primers (Zehr and McReynolds, 1989). In order to minimize the possibility of amplifying contaminants (Zehr *et al.*, 2003), negative controls (autoclaved and ultraviolet-irradiated water) were run with every PCR experiment, reagents were diluted in freshly autoclaved water, the PCR preparation station was ultraviolet irradiated for 1 h before each daily use and the number of cycles was limited to 30 for each reaction. The PCR reagents except for the primers were also irradiated. Each reagent was then tested separately for amplification in negative controls.

Amplified fragments were electrophoresed on 1.2% agarose gels and *nifH* bands were excised and then cleaned using a QIAquick Nucleotide Removal Kit (Qiagen). Cleaned fragments were inserted into a pCR 2.1-TOPO vector using the One Shot TOP10 Chemically Competent *E. coli*, TOPO TA Cloning Kit (Invitrogen) according to the manufacturer's specifications. This resulted in a total of 10 clone libraries, a DNA and a cDNA library from each depth.

Clones were picked randomly and amplified using M13 Forward (−20) and M13 Reverse primers. The products were sequenced at the Macrogen DNA Analysis Facility using Big Dye terminator chemistry (Applied Biosystems, Carlsbad, CA, USA). Sequences were edited using FinchTV ver. 1.4.0 (Geospiza Inc., Seattle, WA, USA) and checked for identity using BLAST. Consensus *nifH* sequences (359 bp) were translated to amino acid (aa) sequences (108 aa after trimming the primer region) and aligned using ClustalX (Thompson *et al.*, 1997) along with published *nifH* sequences from the NCBI database. Neighbor-joining trees were produced from the

alignment using distance matrix methods (PAUP 4.0, Sinauer Associates, Sunderland, MA, USA). Bootstrap analysis was used to estimate the reliability of phylogenetic reconstruction (1000 iterations). The *nifH* sequence from *Methanosarcina lacustris* (AAL02156) was used as an outgroup. The new ETNP *nifH* sequences have been deposited in GenBank, DNA sequence accession numbers KY967751-KY967929 and cDNA sequence accession numbers KY967930-KY968089.

Results

Hydrography

An oxygen-deficient zone was present at all the stations sampled. Based on measurements made with the STOX sensor at the same stations on the same cruise (Tiano *et al.*, 2014), the water column < 60 m at the inshore stations and < 100 m at the offshore stations to a depth of 700–800 m can be considered functionally anoxic (O_2 concentration < 100 nM). Nitrite was detectable in the anoxic layers and the highest NO_2^- concentration (7 μM) occurred at 100 m at a coastal station (Station BB1, Cast 110; Peng *et al.*, 2015). Highest NO_2^- and NO_3^- concentrations were found in the anoxic layers; both were depleted to submicromolar levels in surface waters. The depth distribution of hydrochemistry is shown for depths at which incubations were performed in the coastal region (Stations BB1, 103, 134; Figure 2a) and offshore region (Stations BB2, 163, 168, 173, 179; Figure 2b).

N_2-fixation rates

BNF was ADL in 7 of the 9 surface (2–4 m) samples (ADL = red symbols in Figures 2a and b) with a maximum rate of 3.3 nM day^{-1}. When ADL, BNF in surface waters averaged 2.9 (s.d. = 0.57) nM day^{-1} at the coastal stations and 0.39 (s.d. = 0.12) nM day^{-1} at the offshore stations. The highest BNF rates were found at the coastal stations in the upper 20 m (Figure 2a). The highest recorded rate of 4.3 nM day^{-1} was measured in water samples collected from 20 m at coastal station 108. BNF was ADL in 5 out of 18 ODZ incubations (mean = 0.79, s.d. = 0.48 nM day^{-1}) and did not differ between offshore and nearshore stations. The maximum rate detected at ODZ depths was 1.7 nM day^{-1} at 200 m at Station 134, and the other four ADL rates in the ODZ were < 0.6 nM day^{-1} (Figure 2).

The highest BNF rates were associated with the lowest concentrations of nitrite and nitrate, that is, in surface waters (Figure 2). BNF rates within the anoxic waters were lower than in the surface waters and were usually below the detection limit. The error bars in Figure 2 represent the s.d. of three biological replicates (that is, water collected in three separate Niskin bottles), and they suggest considerable variability or small-scale patchiness in the rates.

nifH diversity

Three hundred and forty-three DNA and cDNA *nifH* sequences were obtained from the 10 clone libraries. The majority of the sequences grouped in Cluster I (Table 1) and a large number of sequences grouped in Clusters III and IV (Table 1).

Cluster I

Samples from all depths from both Stations BB1 and BB2 contained sequences affiliated with Cluster 1 (Figure 3a). A large number of both cDNA and DNA sequences grouped (nt identities between 87% and 90%) with *Methylocystis rosea*, a novel methanotroph that was isolated from Arctic wetland soil. In this alpha Proteobacterial cluster, there were > 50 sequences from all the three depths at Station BB1, along with sequences from the Arabian Sea ODZ (Jayakumar *et al.*, 2012). However, the only cDNA sequences in this group were obtained from a sample collected from oxic waters at the depth of the chlorophyll maximum and the ODZ depth, both from BB1. Within the alpha Proteobacterial cluster is a subgroup containing sequences from several low oxygen environments, including the Arabian Sea and ETSP ODZs, the South China Sea, mangrove sediments and Great Sippewisset Marsh (MA, USA), but none from the ETNP ODZ samples collected here, nt identities between 92% and 100%.

Very few sequences grouped in the beta Proteobacterial cluster, but there was no clear separation between the alpha and beta Proteobacterial groups. Six of the nine ETNP sequences in this cluster, plus one sequence obtained from ETSP upwelling region (Fernandez *et al.*, 2015), are related to *Sinorhizobium meliloti*, an alpha Proteobacterium with nt identities between 68 and 72%. The other three ETNP sequences do not cluster with any cultured bacteria, so we cannot determine whether they belong to the beta or alpha Proteobacterial group.

Thirty-eight DNA and 57 cDNA sequences fell within the gamma Proteobacterial group (Figure 3a). One sequence from the coastal Station BB1 surface sample had high identity with *Vibrio diazotrophicus*, a gamma Proteobacterium associated with marine cyanobacterial mats (Zehr *et al.* unpublished). Many of the sequences in this study that clustered in the gamma Proteobacterial group had no close identities to any cultured gamma Proteobacteria but had close identities to sequences derived from the Arabian Sea ODZ and North Pacific gyre. However, several DNA and cDNA sequences from surface samples from both stations and the ODZ depth of BB2 clustered with *P. stutzeri* and *P. azotifigens* (90–91% nt identities). Two DNA sequences from the surface waters and one cDNA sequence from BB2 ODZ depth had high identities to sequences associated with copepods and sequences derived from microbial mats on a sandy intertidal beach on a Dutch barrier island. Several DNA and cDNA sequences from BB2 surface sample were closely related to sequences
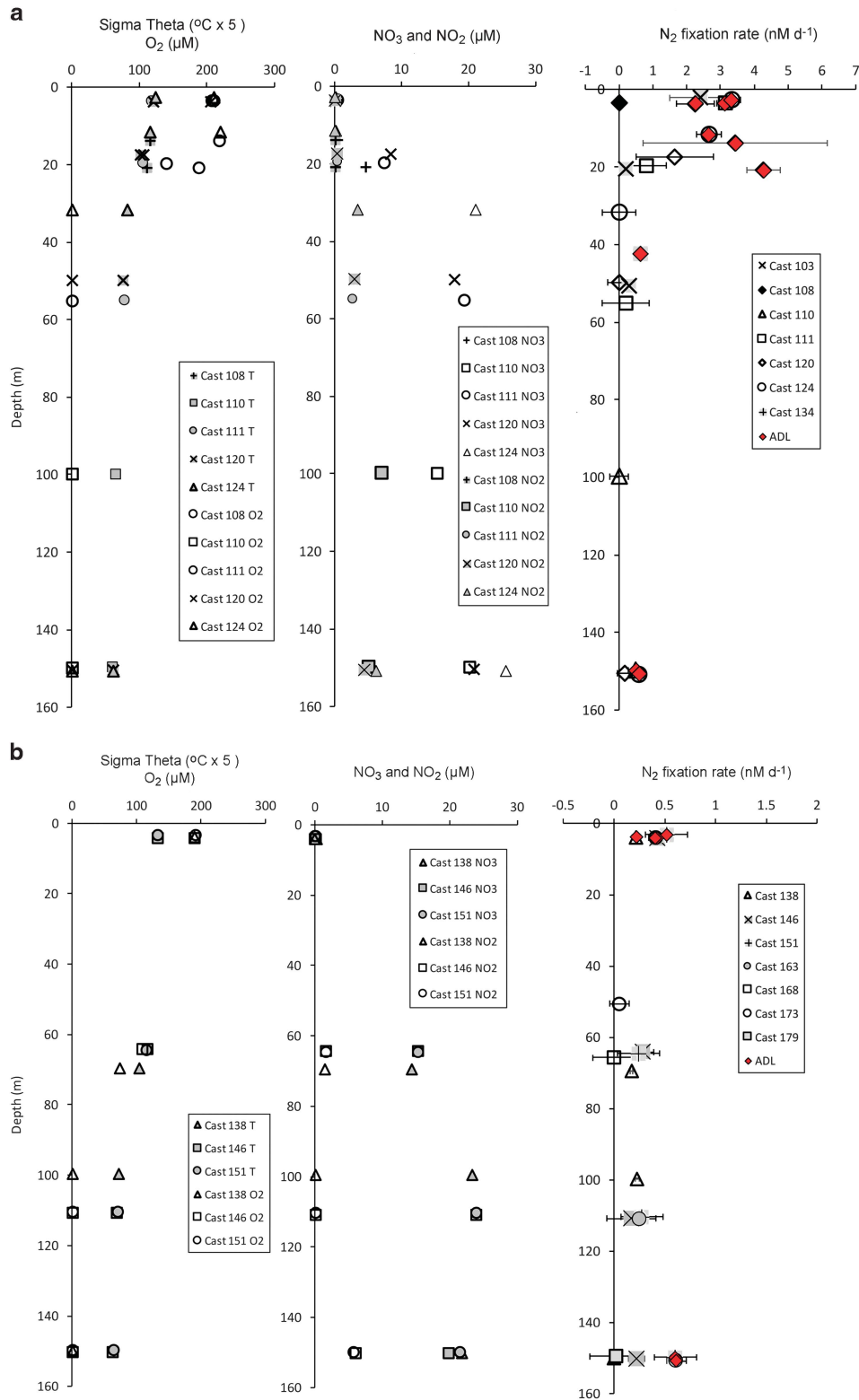
Figure 2 Hydrochemical data and BNF rates at inshore (**a**) and offshore (**b**) stations. Red symbols indicate rates that were significantly ADL. All other rates were not significant.

derived from the South Pacific Gyre (Halm *et al.* (2012); Turk-Kubo *et al.* (2014) and Arabian Sea Bird *et al.* (2005). Eight sequences from BB2 surface sample were closely related to *nifH* sequences from

axenic cultures of *Marichromatium purpuratum* (Braun *et al.*, 1999), obtained from enrichments with planktonic invertebrates. Sequences derived from Arabian Sea were also closely related to this group.

Table 1 *nifH* sequence distribution

Group	DNA	cDNA	Depths
Cluster I	126	86	BB1-0M BB1-18M BB1-90M BB2-0M BB2-150M
Alphaproteobacteria	78	25	BB1-0M BB1-18M BB1-90M BB2-0M BB2-150M
Betaproteobacteria	8	1	BB1-90M BB2-0M BB2-150M
Gammaproteobacteria	38	57	BB1-0M BB2-0M BB2-150M
Deltaproteobacteria	2	0	BB1-0M BB2-0M
Cyanobacteria	0	3	BB2-0M
Cluster II	0	0	None
Cluster III	23	1	BB1-0M BB1-90M BB2-0M
Cluster IV	33	74	BB1-90M BB2-150M
Total	182	161	

However, no sequences with high identities to *Azotobacter vinelandii* were detected in this study, although those were found in the Arabian Sea ODZ (Jayakumar *et al.*, 2012).

Three cDNA sequences identical to *Trichodesmium erythraeum* were found in surface water samples from Station BB2. These had 98% nt identities to the uncultured *Trichodesmium* clones reported by Church *et al.* (2005) that were used to design the most widely used quantitative PCR assay for *Trichodesmium*. No sequences with high identities to any other cyanobacteria were found. Two DNA sequences from the same sample were very closely related to sequences derived from a number of environments, including Chesapeake Bay water, soil, intertidal microbial mat and other marine environments. A subgroup within this cluster had close identities to sequences from the Arabian Sea ODZ and *Geobacter* species. On the basis of affinity to *Geobacter*, we assigned this subgroup to the delta Proteobacteria.

Clusters II, III, and IV

No sequences from samples collected in the ETNP as part of this study grouped in Cluster II. In Cluster III, two sequences from the coastal Station BB1 at the depth of the SNM had 100% identity to a sequence obtained from the Montgri Coast of Spain in the Mediterranean Sea (Ribes *et al.*, 2015; Figure 3b).

Another sequence from the SNM at Station BB1 was closely related (83% nt identities) to a sequence derived from water collected near the Great Barrier Reef. This cluster also contained two sequences from the Verrumicrobiae group (*Opitutaceae bacterium*, isolated from Termite gut, implying the ability to break down cellulose, and *Verrucomicrobiae bacterium* DG1235). Bacteria in this phylum are usually found in eutrophic environments.

Two cDNA sequences from the ODZ (the SNM) at the coastal Station BB1 were quite distinct from each other but grouped in Cluster IV with *Leptolyngbya boryana* IAM M-101, an N_2-fixing cyanobacterium (Fujita *et al.*, 1991; Figure 3b). However, Cluster IV *nifH* sequences encode chlorophyllide reductases and are not nitrogen-fixing genes but are found in cyanobacteria. Four sequences from the SNM at both BB1 and BB2 clustered with sequences (53% nt identities) from an uncultured soil bacterium (Berthrong *et al.*, 2014), and several cDNA sequences from the SNM samples clustered with *Desulfitobacterium hafniense*, a spore-forming anaerobic bacterium.

Discussion

In order to determine the relative magnitude of N inputs in surface and aphotic waters and with respect to gradients in oxygen concentrations, BNF was measured in vertical profiles in the ETNP above, within and below the ODZ. The highest N_2-fixation rates were measured in surface waters but ADL rates were also detected in a few samples collected from ODZ depths.

In order to compare the magnitude of BNF in relation to N loss processes and to evaluate the significance of BNF in aphotic waters, it is first necessary to obtain accurate estimates of BNF rates. The most widely used method for measuring BNF, the 'bubble' method, can yield underestimates of N_2 fixation (Mohr *et al.*, 2010), which can have major implications for balancing the marine N budget (Großkopf *et al.*, 2012). Großkopf *et al.* (2012) calculated that the conventional bubble method leads to an underestimation of global N_2-fixation rates by about a factor of two. In a direct comparison of the bubble method (in which the tracer is added as a bubble of $^{15}N_2$ gas) versus the 'dissolution' method (in which the tracer $^{15}N_2$ is preequilibrated in filtered and degassed sea water and then added to the incubation), the dissolved tracer additions resulted in 2–3.5-fold higher N_2-fixation rates than the bubble method (Wilson *et al.*, 2012). The method we used was designed to overcome limitations of both approaches. The main problem with the bubble method is that full isotopic equilibration between the $^{15}N_2$ tracer and ambient N_2 in incubated seawater is assumed right from the beginning of the incubation. In practice, however, the bubble does not equilibrate completely with the aqueous phase N_2, even over the course of a 24-h incubation, leading to an overestimate of the isotopic enrichment of the
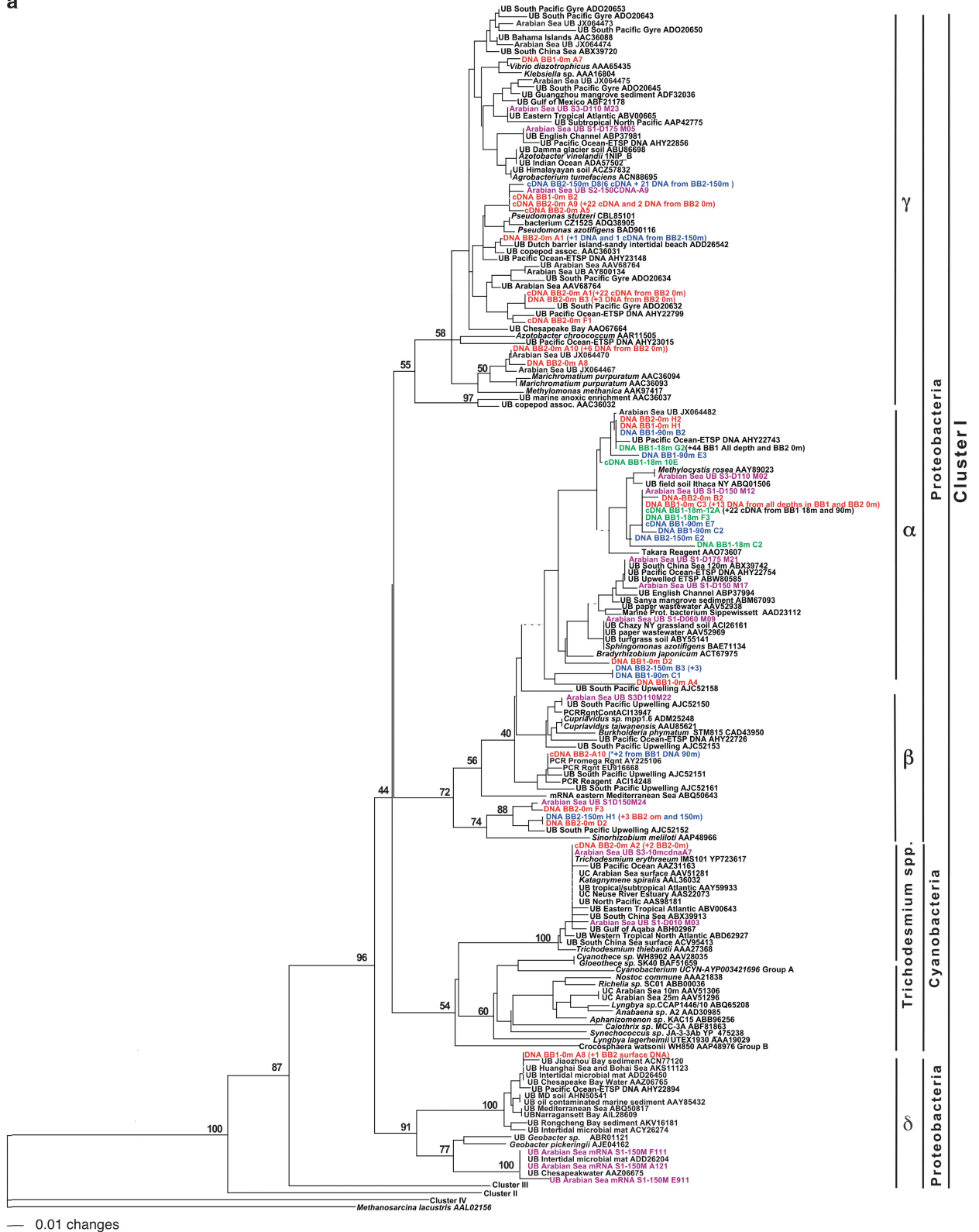
a

Figure 3 Phylogenetic trees of *nifH* sequences. DNA and cDNA sequences from the current study are highlighted in color with the clone number at the end and coded for depth: surface samples in red, chlorophyll maximum depth in green and ODZ depths in blue and from the Arabian Sea OMZ region in magenta (Jayakumar *et al.*, 2012). Sequences from other studies are in black, with the NCBI Accession number at the end. UB = uncultured bacterium. (**a**) *nifH* phylogeny within *nifH* Cluster I. (**b**) *nifH* phylogeny within Clusters II, III and IV.

b

Figure 3 (continued).

dissolved N_2 pool and an underestimate of the calculated BNF rate (see Equation 1). The dissolution method requires substantial time and manipulation to filter, degas and preequilibrate site water with

$^{15}N_2$, and it is almost impossible to generate sufficient quantities of enriched water that has the unique physical and chemical properties of each water sample in a reasonable amount of time.

The preparation of enriched seawater requires degassing, which changes, among other things, the carbonate chemistry and pH by outgassing of carbon dioxide. Its addition to sample incubation bottles has unknown effects on the microbial community. For ODZ samples, there is the added complication of oxygen contamination.

To avoid the limitations of the bubble method, we adopted a modified bubble method to measure the rates of BNF in the ETNP. Highly enriched tracer was added to incubations as a bubble, but the amount of isotope enrichment over time was directly measured in parallel incubations so that the actual substrate enrichment was known. Avoiding preequilibration steps allowed us to initiate the incubations rapidly upon sample collection and monitoring the actual tracer enrichment allowed us to calculate the $^{15}N_2$-uptake rates more accurately. In addition, the rigorous determination of detection limit for each individual rate measurement, as applied here, may support more robust conclusions than was possible in some earlier reports.

Contamination of the tracer $^{15}N_2$ gas has recently been identified as another potential source of artifact in the measurement of N_2-fixation rates (Dabundo *et al.*, 2014). We calculated the N_2-fixation rate that would have been inferred from the uptake of ^{15}N contaminants using the finite-differencing model approach of Dabundo *et al.* (2014), assuming the highest level of contamination found in lots from Cambridge Isotopes (0.052 µmol $^{15}NH_4^+$ per mole $^{15}N_2$; Dabundo *et al.*, 2014), in conjunction with the measured values of nutrients and particulate nitrogen concentration found in this study (additionally assuming ambient $\delta^{15}N\text{-}NH_4^+ = -2$‰ and a specific growth rate coefficient of 0.3 day^{-1}). The rates of N_2 fixation inferred from the potential uptake of ^{15}N contaminants ranged from undetectable to 0.019 nmol $N^{-1} l^{-1} day^{-1}$, averaging 0.008 nmol $N^{-1} l^{-1} day^{-1}$. This was ⩽7% of the magnitude of detectable N_2-fixation rates measured in this study (average 2%), indicating that the ^{15}N enrichment of particulate nitrogen observed in this study was overwhelming from N_2 fixation and not the uptake of ^{15}N contaminants.

N_2-fixation rates have been reported from several recent investigations of N cycling in OMZs that employed the standard bubble method of tracer addition. In waters offshore of the OMZ in the ETSP, BNF rates were highest in surface waters (up to 0.9 nM day^{-1}) and rates of up to 0.6 nM day^{-1} were detected in low O_2 deep water (600 m) (Bonnet *et al.*, 2013; Dekaezemacker *et al.*, 2013; Turk-Kubo *et al.*, 2014). Loscher *et al.* (2014) reported very high BNF rates (~25 nM day^{-1}) in surface waters at a eutrophic coastal station in the ETSP and nearly 10 nM day^{-1} in the sulfidic bottom water at that station. Similarly, high rates of N_2 fixation were observed in surface waters in the coastal North Atlantic Ocean (Mulholland *et al.*, 2012). However, not only are these rates likely underestimates based on the methodological considerations outlined above but

might also be usefully re-evaluated with stricter detection limits.

The BNF rates reported here are among the first from the ETNP ODZ so it is useful to compare them with those from the ETSP and elsewhere. White *et al.* (2013) reported low integrated N-fixation rates (based on the bubble method) in the surface layer at two stations in the region of the current study, but it is difficult to make direct comparisons because depth profiles were not provided and the ODZ depths were not sampled. Surface waters from the coastal Station BB1 (total depth 2330 m) were less eutrophic than the sulfidic coastal station in the ETSP occupied by Loescher *et al.* (2014). The open ocean Station BB2 sampled in this study was within the ETNP ODZ. In contrast, Bonnet *et al.* (2013) sampled the outer edge of the ODZ in the ETSP. Surface BNF rates measured at Station BB1 were higher than those measured further offshore in the ETSP (Bonnet *et al.*, 2013) but lower than those observed at the coastal ETSP site (Loescher *et al.*, 2014). BNF rates measured at Station BB2 were the same order of magnitude as those from the offshore ETSP station (Bonnet *et al.*, 2013) and comparable to rates measured in samples collected at 40 m at a nearshore station in the ETSP (Loescher *et al.*, 2014) and hypoxic waters of the Southern California Bight (0.07–0.25 nM day^{-1}; Hamersley *et al.*, 2011). Although the rates reported here for the ETNP may be more accurate than those obtained with the standard bubble method, they are not substantially different in magnitude. The rates reported here are within the range of those reported previously for ODZs and lower than those reported for surface waters. BNF rates in the coastal surface waters were comparable to rates measured in coastal surface waters in the ETSP and elsewhere (Mulholland *et al.*, 2012) and so represent a previously unquantified source of fixed N.

Denitrification and anammox rates have been reported previously for samples collected at the same stations during this cruise (Babbin *et al.*, 2014). Total N loss rates were highest near the top of the ODZ and decreased with increasing depth in accordance with the Martin curve (Martin *et al.*, 1987). Maximum N loss rates of nearly 30 nM N day^{-1} were observed at the coastal Station BB1 at 60 m and rates of ~ 10 nM N day^{-1} occurred near 100 m at both Stations BB1 and BB2. In contrast, maximum BNF rates occurred in the euphotic zone in the upper 20 m, much shallower than the depth of the maximum in N loss rates. At depths in the core of the ODZ (>60 m at BB1 and >100 m at BB2), volumetric N loss rates exceeded BNF rates by a factor of ~ 20.

Because reliable oxygen concentration measurements are sparse, we took the approach of Babbin *et al.* (2015), who used a corrected World Ocean Atlas dissolved oxygen database and set the dissolved oxygen definition for ODZ waters at 2.5 µM. By this definition, the volume of the anoxic water in

the ETNP was estimated to be $1.2 \pm 0.5 \times 10^{15}$ m^3. The average of ADL rates in the ODZ (0.79 nM day^{-1}) was multiplied by this volume of water to yield an estimate of 0.1 Tg N year^{-1} for the total BNF rate in the anoxic waters of the ETNP. However, this value should be considered an upper limit because it does not include zero values for BNF observed in most incubations in the ODZ. For perspective, the global water column BNF rate is estimated to be 140 Tg N year^{-1} (Deutsch *et al.*, 2007). The measured anoxic BNF rates suggest that N$_2$ fixation in the ODZ of the ETNP is not a significant contribution to the global N budget. The global water column denitrification rate is estimated at 70 Tg N year^{-1} (Devries *et al.*, 2012). If the ETNP region accounts for 30% of the global water column N loss (21 Tg N year^{-1}), our estimated maximum anoxic BNF rate for the ETNP of 0.1 Tg N year^{-1} could not significantly offset that loss.

The main conclusion from the present study is that, even with improved incubation methods, sensitive mass spectrometry, careful replication and robust statistical analysis, BNF rates are low in the ETNP in both surface and anoxic waters. The data set we report here is small and highly variable and so a more comprehensive examination of N$_2$ fixation in oxygen-deficient waters is necessary before concluding that anoxic BNF is not a significant component of the N cycle.

As in the current study, most of the *nifH* sequences from the ETSP aphotic/anoxic waters were associated with Cluster I and affiliated with various branches of the Proteobacteria (Bonnet *et al.*, 2013; Loescher *et al.*, 2014; Turk-Kubo *et al.*, 2014). However, unlike the Arabian Sea, a large number of sequences from the ETNP ODZ also grouped in Clusters III and IV.

Similar to the ETNP, diverse gamma Proteobacteria were found in the ETSP (Turk-Kubo *et al.*, 2014), but quantitative PCR assays indicated that their abundance was too low to account for the measured BNF rates there. These authors argued that, despite the diversity of novel diazotrophs in subsurface waters, the agents responsible for the measured BNF remain unidentified and possibly so divergent as to have avoided detection so far.

Despite the fact that the highest BNF rates were found in surface waters, we retrieved very few *nifH* sequences affiliated with known cyanobacterial N$_2$ fixers. Only three *Trichodesmium* sequences were found in the offshore surface sample even though this ubiquitous group is found almost everywhere in the subtropical surface ocean. Similarly, Turk-Kubo *et al.* (2014) detected only three cyanobacterial phylotypes in the ETSP, including a novel *Trichodesmium* type, which accounted for only 4% of the sequences in their clone libraries and could not be quantified by quantitative PCR. In the present study, it was not possible to distinguish heterotrophic from cyanobacterial N$_2$ fixation in surface waters. Although cyanobacterial diazotrophs are generally

the targets for quantitative PCR in surface waters, heterotrophic diazotrophs are also retrieved in clone libraries of surface water samples and may contribute to BNF in the euphotic zone (Mulholland *et al.*, 2012). Amplification and/or cloning bias depending on the PCR primers cannot be discounted as part of the reason for low detection of cyanobacterial *nifH* sequences, but low rates and low cyanobacterial abundance are consistent with a relatively minor role for of N fixation in this region. In the region of the stations sampled here, White *et al.* (2013) detected low numbers of *Trichodesmium* filaments and low abundance of the cyanobacterial-symbiont-bearing diatom, *Richelia*. White *et al.* (2013) also concluded that diazotrophy was a relatively minor contribution to the N budget and to sinking particulate flux.

The highest BNF rates in the ETNP were detected in surface waters where fixed N concentrations were very low. It does not appear, however, that fixed N availability is the major control variable on BNF, as has been observed in the coastal Atlantic Ocean (Mulholland *et al.*, 2012). In the present study, we detected active BNF in dissolved inorganic nitrogen-replete (> 20 μM) aphotic waters below the nitracline (Figure 2). The main diazotrophs detected in this region, in both surface and deep waters, both oxic and anoxic conditions, were Proteobacteria, presumably mainly heterotrophic. Why N fixation would be advantageous over assimilation of dissolved inorganic nitrogen or dissolved organic nitrogen is unknown.

Similarly, while low oxygen concentrations are thought to be favorable for BNF, we measured the highest BNF rates in oxic surface waters. Our results are consistent with other recent studies in suggesting that the habitat for diazotrophy includes dark deep water replete with fixed N (Rahav *et al.*, 2013; Loescher *et al.*, 2014; Turk-Kubo *et al.*, 2014), where BNF is accomplished by diverse heterotrophic diazotrophic assemblages.

Conclusions

Low rates of BNF were detected in both surface and anoxic waters in the ETNP ODZ region. Combined findings of BNF in surface waters and anoxic deep waters of the ETNP, in the ETSP and elsewhere in anoxic waters may warrant a re-evaluation of the global N budget but are unlikely to change it very much. In the ETNP, BNF was apparently conducted by novel bacterial groups in the presence of high concentrations of fixed N, thus emphasizing the need to re-evaluate our understanding of the regulation of BNF in the ocean.

Conflict of Interest

The authors declare no conflict of interest.

Acknowledgements

References

Babbin AR, Bianchi, Jayakumar A, Ward BB. (2015). Rapid nitrous oxide cycling in the suboxic ocean. *Science* **348**: 1127–1129.

Babbin AR, Keil RG, Devol AH, Ward BB. (2014). Organic matter stoichiometry, flux, and oxygen control nitrogen loss in the ocean. *Science* **344**: 406–408.

Berthrong ST, Yeager CM, Gallegos-Graves L, Steven B, Eichorst SA, Jackson RB *et al.* (2014). Nitrogen fertilization has a stronger effect on soil nitrogen-fixing bacterial communities than elevated atmospheric CO$_2$. *Appl Environ Microb* **80**: 3103–3112.

Bird C, Martinez J, O'Donnell A, Wyman M. (2005). Spatial distribution and transcriptional activity of an uncultured clade of planktonic diazotrophic gamma-proteobacteria in the Arabian Sea. *Appl Environ Microb* **71**: 2079–2085.

Bonnet S, Dekaezemacker J, Turk-Kubo KA, Moutin T, Hamersley RM, Grosso O *et al.* (2013). Aphotic N-2 fixation in the Eastern Tropical South Pacific Ocean. *PLos One* **8**: e81265.

Braun ST, Proctor LM, Zani S, Mellon MT, Zehr JP. (1999). Molecular evidence for zooplankton-associated nitrogen-fixing anaerobes based on amplification of the nifH gene. *FEMS Microbiol Ecol* **28**: 273–279.

Church MJ, Jenkins BD, Karl DM, Zehr JP. (2005). Vertical distributions of nitrogen-fixing phylotypes at stn ALOHA in the oligotrophic North Pacific Ocean. *Microb Ecol* **38**: 3–14.

Dabundo R, Lehmann MF, Treibergs L, Tobias CR, Altabet MA, Moisander PH *et al.* (2014). The contamination of commercial N-15(2) gas stocks with N-15-labeled nitrate and ammonium and consequences for nitrogen fixation measurements. *PLos One* **9**: e110335.

Dekaezemacker J, Bonnet S, Grosso O, Moutin T, Bressac M, Capone DG. (2013). Evidence of active dinitrogen fixation in surface waters of the eastern tropical South Pacific during El Nino and La Nina events and evaluation of its potential nutrient controls. *Global Biogeochem Cycles* **27**: 768–779.

Deutsch C, Sarmiento JL, Sigman DM, Gruber N, Dunne JP. (2007). Spatial coupling of nitrogen inputs and losses in the ocean. *Nature* **445**: 163–167.

Devol AH. (2008). Denitrification, including Anammox. In: Capone DG, Bronk DA, Mulholland MR, Carpenter EJ (eds). *Nitrogen in the Marine Environment.* 2nd edn. Elsevier: Amsterdam, The Netherlands, pp 263–301.

Devries T, Deutsch C, Primeau F, Chang B, Devol A. (2012). Global rates of water-column denitrification derived from nitrogen gas measurements. *Nat Geosci* **5**: 547–550.

Fernandez C, Gonzalez ML, Muñoz C, Molina V, Farias L. (2015). Temporal and spatial variability of biological nitrogen fixation off the upwelling system of central Chile (35–38.5°S). *J Geophys Res Oceans* **120**: 3330–3349.

Fernandez C, Farias L, Ulloa O. (2011). Nitrogen fixation in denitrified marine waters. *PLos One* **6**: e20539.

Fujita Y, Takahashi Y, Shonai F, Ogura Y, Matsubara H. (1991). Cloning, nucleotide-sequences and differential expression of the nifH and nifH-like (frxC) genes from the filamentous nitrogen -fixing cyanobacterium *Plectonema boryanum*. *Plant Cell Physiol* **32**: 1093–1106.

Großkopf T, Laroche J. (2012). Direct and indirect costs of dinitrogen fixation in *Crocosphaera watsonii* WH8501 and possible implications for the nitrogen cycle. *Front Microbiol* **3**: 236.

Großkopf T, Mohr W, Baustian T, Schunck H, Gill D, Kuypers MMM *et al.* (2012). Doubling of marine dinitrogen-fixation rates based on direct measurements. *Nature* **488**: 361–364.

Hamersley MR, Turk KA, Leinweber A, Gruber N, Zehr JP, Gunderson T *et al.* (2011). Nitrogen fixation within the water column associated with two hypoxic basins in the Southern California Bight. *Aquat Microb Ecol* **63**: 193-+.

Halm H, Lam P, Ferdelman TG, Lavik G, Dittmar T, LaRoche J *et al.* (2012). Heterotrophic organisms dominate nitrogen fixation in the South Pacific Gyre. *ISME J* **6**: 1238–1249.

Jayakumar A, Al-Rshaidat MMD, Ward BB, Mulholland MR. (2012). Diversity, distribution, and expression of diazotroph nifH genes in oxygen-deficient waters of the Arabian Sea. *FEMS Microbiol Ecol* **82**: 597–606.

Loescher CR, Grosskopf T, Desai FD, Gill D, Schunck H, Croot PL *et al.* (2014). Facets of diazotrophy in the oxygen minimum zone waters off Peru. *ISME J* **8**: 2180–2192.

Martin JH, Knauer GA, Karl DM, Broenkow WW. (1987). Vertex—carbon cycling in the Northeast Pacific. *Deep Sea Res Part A Oceanogr Res Pap* **34**: 267–285.

Mcilvin MR, Casciotti KL. (2010). Fully automated system for stable isotopic analyses of dissolved nitrous oxide at natural abundance levels. *Limnol Oceanogr Methods* **8**: 54–66.

Mohr W, Grosskopf T, Wallace DWR, Laroche J. (2010). Methodological underestimation of oceanic nitrogen fixation rates. *PLos One* **5**: e12583.

Montoya JP, Voss M, Kaehler P, Capone DG. (1996). A simple, high-precision, high-sensitivity tracer assay for N2 fixation. *Appl Environ Microb* **62**: 986–993.

Mulholland MR, Bernhardt PW, Heil CA, Bronk DA, O'Neil JM. (2006). Nitrogen fixation and release of fixed nitrogen by Trichodesmium spp. in the Gulf of Mexico. *Limnol Oceanogr* **51**: 1762–1776.

Mulholland MR, Bernhardt PW, Blanco-Garcia JL, Mannino A, Hyde K, Mondragon E *et al.* (2012). Rates of dinitrogen fixation and the abundance of diazotrophs in North American coastal waters between

Cape Hatteras and Georges Bank. *Limnol Oceanogr* **57**: 1067–1083.

Mulholland MR, Capone DG. (2009). Dinitrogen fixation in the Indian Ocean. In: Wiggert JD, Hood RR, Naqvi SWA, Brink KH, Smith SL (eds). *Indian Ocean Biogeochemical Processes and Ecological Variability*. American Geophysical Union: Washington, DC, USA, pp 167–186.

Peng X, Fuchsman CA, Jayakumar A, Oleyni S, Martens-Habbena W, Devol AH *et al.* (2015). Ammonia and nitrite oxidation in the Eastern Tropical North Pacific. *Glob Biogeochem Cycles* **29**: 2034–2049.

Rahav E, Bar-Zeev E, Ohayon S, Elifantz H, Belkin N, Herut B *et al.* (2013). Dinitrogen fixation in aphotic oxygenated marine environments. *Front Microbiol* **4**: 00227.

Ribes M, Dziallas C, Coma R, Riemann L. (2015). Microbial diversity and putative diazotrophy in high- and low-microbial-abundance mediterranean sponges. *Appl Environ Microb* **81**: 5683–5693.

Santoro AE, Sakamoto CM, Smith JM, Plant JN, Gehman AL, Worden AZ *et al.* (2013). Measurements of nitrite production in and around the primary nitrite maximum in the central California Current. *Biogeosciences* **10**: 7395–7410.

Thamdrup B, Dalsgaard T. (2002). Production of N_2 through anaerobic ammonium oxidation coupled to nitrate reduction in marine sediments. *Appl Environ Microb* **68**: 1312–1318.

Thompson JD, Gibson TJ, Plewniak F, Jeanmougin F, Higgins DG. (1997). The CLUSTAL_X windows interface: flexible strategies for multiple sequence alignment aided by quality analysis tools. *Nucleic Acids Res* **25**: 4876–4882.

Tiano L, Garcia-Robledo E, Dalsgaard T, Devol AH, Ward BB, Ulloa O *et al.* (2014). Oxygen distribution and aerobic respiration in the north and south eastern tropical Pacific oxygen minimum zones. *Deep Sea Res Part I Oceanogr Res Pap* **94**: 173–183.

Turk-Kubo KA, Karamchandani M, Capone DG, Zehr JP. (2014). The paradox of marine heterotrophic nitrogen fixation: abundances of heterotrophic diazotrophs do not account for nitrogen fixation rates in the Eastern Tropical South Pacific. *Environ Microbiol* **16**: 3095–3114.

White AE, Foster RA, Benitez-Nelson CR, Masque P, Verdeny E, Popp BN *et al.* (2013). Nitrogen fixation in the Gulf of California and the Eastern Tropical North Pacific. *Prog Oceanogr* **109**: 1–7.

Wilson ST, Boettjer D, Church MJ, Karl DM. (2012). Comparative assessment of nitrogen fixation methodologies, conducted in the Oligotrophic North Pacific Ocean. *Appl Environ Microb* **78**: 6516–6523.

Zani S, Mellon MT, Collier JL, Zehr JP. (2000). Expression of *nifH* genes in natural microbial assemblages in Lake George, New York, detected by reverse transcriptase PCR. *Appl Environ Microb* **66**: 3119–3124.

Zehr JP, Crumbliss LL, Church MJ, Omoregie EO, Jenkins BD. (2003). Nitrogenase genes in PCR and RT-PCR reagents: implications for studies of diversity of functional genes. *Biotechniques* **35**: 996–1002.

Zehr JP, McReynolds LA. (1989). Use of degenerate oligonucleotides for amplification of the *nifH* gene from the marine cyanobacterium *Trichodesmium theiebautii*. *Appl Environ Microb* **55**: 2522–2526.

Zehr JP, Mellon MT, Zani S. (1998). New nitrogen-fixing microorganisms detected in oligotrophic oceans by amplification of nitrogenase (nifH) genes. *Appl Environ Microb* **6**: 3444–3450.

Zehr JP, Montoya JP, Jenkins BD, Hewson I, Mondragon E, Short CM *et al.* (2007). Experiments linking nitrogenase gene expression to nitrogen fixation in the North Pacific subtropical gyre. *Limnol Oceanogr* **52**: 169–183.

Supplementary Information accompanies this paper on The ISME Journal website (http://www.nature.com/ismej)